Title

Chemical Control of Plasmons in Metal Chalcogenide and Metal Oxide Nanostructures

Journal

Advanced Materials, 27(38)

ISSN

0935-9648

Authors

Mattox, Tracy M

Ye, Xingchen

Manthiram, Karthish

et al.

Publication Date

2015-10-01

DOI

10.1002/adma.201502218

Peer reviewed

ADVANCED MATERIALS
www.advmat.de

Chemical Control of Plasmons in Metal Chalcogenide and Metal Oxide Nanostructures

*Tracy M. Mattox, Xingchen Ye, Karthish Manthiram, P. James Schuck, A. Paul Alivisatos, and Jeffrey J. Urban**

The field of plasmonics has grown to impact a diverse set of scientific disciplines ranging from quantum optics and photovoltaics to metamaterials and medicine. Plasmonics research has traditionally focused on noble metals; however, any material with a sufficiently high carrier density can support surface plasmon modes. Recently, researchers have made great gains in the synthetic (both intrinsic and extrinsic) control over the morphology and doping of nanoscale oxides, pnictides, sulfides, and selenides. These synthetic advances have, collectively, blossomed into a new, emerging class of plasmonic metal chalcogenides that complement traditional metallic materials. Chalcogenide and oxide nanostructures expand plasmonic properties into new spectral domains and also provide a rich suite of chemical controls available to manipulate plasmons, such as particle doping, shape, and composition. New opportunities in plasmonic chalcogenide nanomaterials are highlighted in this article, showing how they may be used to fundamentally tune the interaction and localization of electromagnetic fields on semiconductor surfaces in a way that enables new horizons in basic research and energy-relevant applications.

1. Introduction

Metal chalcogenide and metal oxide nanoparticles represent a new and intriguing class of plasmonic materials. In contrast to noble metals, these materials are capable of localizing light on a broad variety of semiconductor surfaces, while also presenting new methods for plasmon control, such as doping. Thus, these materials nicely complement classical plasmonic materials such as Ag, Au, and Cu, which possess enormous free carrier densities and exhibit sharp localized surface plasmon resonance (LSPR) modes.

The field of noble metal plasmonics is vast,[1] which reflects the tremendous impact and unique role that these types of plasmons play in state-of-the-art applications such as photovoltaics,[2] medicine,[3] and quantum optics.[4] In particular, great synthetic control over noble metal nanoparticles has enabled the design of materials with resonances that span from the UV (Ag nanospheres)[5] to the IR (Au nanoshells).[6] Non-noble metal materials have the potential to further expand plasmonic functionality and tunability. However, the primary downside of these materials has been, and in many cases continues to be, the lossy nature of their plasmon resonances, which limits their use in certain applications. In an important development for non-noble metal plasmonics, researchers have recently demonstrated metal-oxide plasmons with Q-factors as large as those achieved in noble metal nanoparticles;[7] this finding opens up new possible applications for these materials and complements what is already known about noble metal plasmonics. In this article, we concentrate solely on metal chalcogenides and metal oxides, focusing on the chemical, synthetic, and mechanistic means to control plasmons in this fascinating class of materials.

The position of the LSPR absorbance band in the optical spectra may be controlled by changing the carrier density n or in a complementary fashion by introducing vacancies, such as copper deficiencies in copper(I) sulfides in the early work of Zhao et al.[8] The detailed physical chemistry of how defect activation and compensation relates to plasmonic and optoelectronic properties is discussed in recent reviews by Faucheaux et al.[9] on semiconductor nanocrystals and Lounis et al.[10] on oxide materials. Detailed summaries of the plasmonics of heavily doped semiconductors are discussed in additional reviews by Scotognella et al.[11] and Liu and Swihart.[12]

The ability to dope plasmonic materials greatly expands the accessible absorbance range to include the visible, near-infrared (NIR), and mid-infrared regions, offering a much larger range of dielectric constants than previously available and dramatically expanding the spectral breadth of plasmonics (**Figure 1**). This wider absorbance range is opening new doors to researchers, making it possible to develop, for instance,

T. M. Mattox, Dr. P. J. Schuck, Dr. J. J. Urban
The Molecular Foundry
Lawrence Berkeley National Laboratory
Berkeley, CA 94720, USA
E-mail: jjurban@lbl.gov
Dr. X. Ye, Dr. A. P. Alivisatos
Department of Chemistry
University of California
Berkeley, CA 94720, USA
Dr X. Ye, Dr. K. Manthiram, Dr. A. P. Alivisatos
Materials Sciences Division
Lawrence Berkeley National Laboratory
Berkeley, CA 94720, USA
Dr. K. Manthiram
Department of Chemical and Biomolecular Engineering
University of California
Berkeley, CA 94720, USA

DOI: 10.1002/adma.201502218

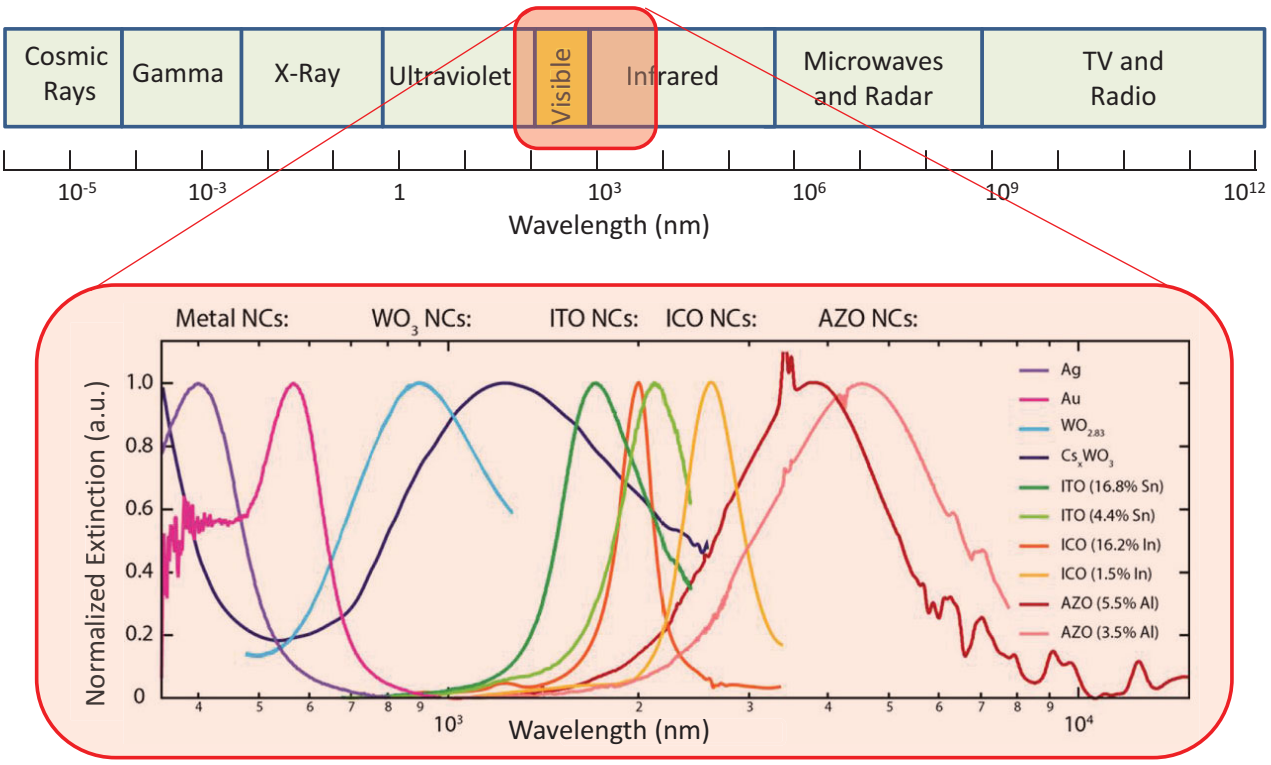

Figure 1. Electromagnetic spectrum and absorbance spectra of metal and chalcogenide plasmonic materials spanning multiple frequencies. All materials are spherical in shape with the exception of $WO_{2.83}$ rods. Reproduced with permission.[10] Copyright 2014, American Chemical Society.

electrochromic smart windows that darken at the flip of a switch[13,14] and window coatings that absorb solar heat while remaining transparent.[15] An in-depth treatment of the fundamental physical considerations that govern plasmon location, breadth, and decay in these chalcogenide and metal-oxide materials is covered in a recent review by Comin and Manna.[16]

Particle morphology is another important avenue for tuning the LSPR, and it is established for noble metals that changing the size and shape will influence the resonant frequency.[17] Only recently have metal chalcogenides of varying shapes been developed, such as doped tungsten oxide (prisms, cubes and spheres)[15] and copper telluride (plates, cubes and rods).[18] Recent work by Agrawal et al.[19] highlights the importance of morphology by calculating the influence of *n* on the LSPR of an indium doped cadmium oxide (ICO) sphere, cube, rounded cube, and octahedron.[19] Varying the particle morphology within the same system allows researchers to make shape comparisons with respect to LSPR that were previously only possible in noble metals, which enables the development of new classes of devices with plasmon-enhanced functionalities spanning multiple frequencies in the electromagnetic spectrum.

In this article, we focus on recent developments in controlling the LSPR of metal chalcogenides and metal oxides. The wide range of controls now available to tune the plasmon is immense, and enables new ways to manipulate the fundamental metal-optics levers of carrier mobility, density, and interband losses. We focus on how chemical controls, hierarchical structuring, self-assembly, and post-synthesis modulation may be used as fundamental levers to manipulate plasmonic responses in materials beyond more conventional approaches.

2. Shape Control of Nanoparticle Plasmons

Nanocrystal shapes provide the boundary conditions for surface plasmons, and can be used to manipulate the frequency of the plasmons. In noble metals, the morphology of nanoparticles has a strong influence on the shape and position of the plasmon absorbance. This is also the case with plasmonic metal chalcogenides and metal oxides, with the added benefit of another degree of freedom for further tuning the plasmon through doping to modulate the carrier concentration. In addition to this, anisotropic structures may support multiple plasmon modes along different directions having distinct energies. These plasmonic modes can be further amplified or made silent by coupling the modes of individual particles together or with metallic plasmons in hierarchically ordered assemblies. To help illuminate the importance of particle shape on LSPR, we describe here the most recent synthetic techniques developed to create varying shapes of plasmonic metal chalcogenides and metals oxides.

2.1. Colloidal Chemistry Routes to Shape Control

2.1.1. Copper Telluride Plates, Cubes and Rods (ca. 900 nm absorbance)

Li et al. recently reported that the plasmon of copper telluride (CuTe)[18] results from Cu vacancies, and the nanoparticles have a LSPR extinction cross section higher than that found in plasmonic metals. The Cu:Te ratio, reaction time, temperature, and

Adv. Mater. **2015**,
DOI: 10.1002/adma.201502218

ligand concentration all help control the shape. As the morphology of CuTe changes from cubes to plates to thin rods, the intensity of the LSPR peak at ca. 900 nm decreases and nearly disappears for the rods. The author reports that the weak intensity of thin nanorods is likely because the small transverse dimension, or "thickness", of the rod does not support a detectable plasmon. It is also possible that plasmons in these systems may be highly lossy.

Kriegel et al. also discuss copper chalcogenides in three distinct morphologies; spheres, rods, and tetrapods.[20] Interestingly, the shape dependence of the extinction spectra of $Cu_{2-x}Te$ is very weak, while in strongly plasmonic noble metals, such as Au[21] and Ag,[22] the shape-effect is much more dramatic. This is believed to be a consequence of strong electric fields being so sensitive to the shape of the nanoparticle and boundary conditions.

2.1.2. Cesium Tungstate Hexagonal Prisms, Truncated Cubes, and Pseudo-Spheres (ca. 800 and 1600 nm Absorbance)

In contrast to Cu vacancies, cesium tungstate (Cs_xWO_3)[15] is plasmonic as a result of interstitial doping, where Cs^+ ions are positioned in the defect-induced (oxygen-vacancy) channels of tungsten oxide. Mattox et al.[15] report the synthesis of Cs_xWO_3 as phase-pure, monodisperse nanoparticles; hexagonal prisms, truncated cubes, and pseudo-spheres. These nanocrystals exhibit strongly shape-dependent LSPR features in the near-infrared (NIR) region. This material follows the same trends reported for the truncations of silver cubes, where increasing the number of faces or planes on the surface forces the plasmon peaks closer together.[17] As the shape of Cs_xWO_3 nanocrystals changes from hexagonal prisms (8 faces), to truncated cubes (10 faces), to pseudo-spheres (infinite faces), the two distinct optical peaks at 860 nm and 1602 nm reduce to one observable peak at 1315 nm (**Figure 2**A). As the number of faces on the nanoparticle surface increases, three important trends are apparent: i) the main/largest resonance peak blue-shifts, ii) smaller peaks move closer to the main peak and may be hidden, and 3) the width of the main resonance peak increases.[15,17]

The same trends are observed when decreasing the aspect ratio (length over width) of plasmonic nanoparticles, where the plasmon peaks shift closer together. In rod-shaped noble metals (e.g., Au[21] and Ag[22]), the plasmon mode of the longer axis is typically well defined and easy to observe due to strong coupling to the electromagnetic field. This is in contrast to $WO_{2.8}$ nanorods described by Manthiram and Alivisatos, which have a high aspect ratio yet the long-axis mode is difficult to observe.[23] According to calculations, the plasmon resulting from the longer axis occurs at low energies and is rather broad.[23]

2.1.3. Copper Sulfide ($Cu_{2-x}S$) Disks (ca. 1700 and 3600 nm Absorbance) and Hexagonal Disks (ca. 900 and 1300 nm Absorbance)

The plasmon of copper sulfide ($Cu_{2-x}S$) results from holes introduced by Cu vacancies, as reported by Hsu et al.,[24] where the $Cu_{2-x}S$ nanodisks have plasmons in the NIR region (ca. 1700 nm and ca. 3600 nm). Disk-shapes have two planes, commonly labeled "in-plane" and "out-of-plane" (Figure 2B), where each plane is responsible for a LSPR mode in the absorbance spectra. In $Cu_{2-x}S$, the aspect ratio (diameter over thickness) may be tuned from 4.65 to 7.10 by changing the oxygen content and reaction time. As seen in this system, changing the aspect ratio is a means of controlling the plasmon. Increasing the aspect ratio causes the out-of-plane plasmon to blue-shift and the in-plane to red-shift, which is in agreement with conventional Mie scattering theory.[25]

Xie et al. describe that unlike the traditional plasmonic chalcogenides mentioned above, copper sulfide (CuS) is reluctant to incorporate cation vacancies due to the slow diffusion of

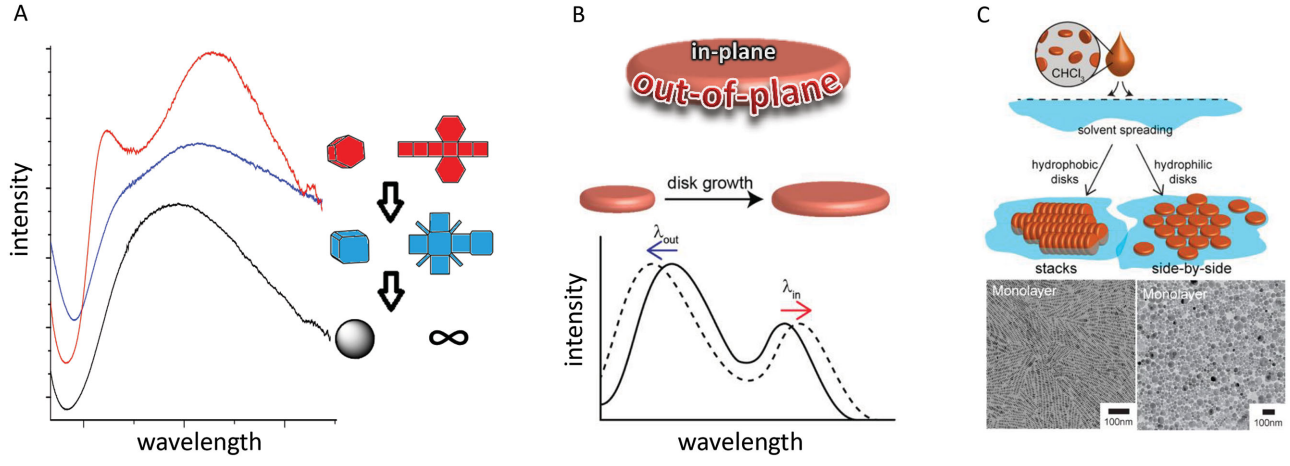

Figure 2. A) Absorbance spectra of Cs_xWO_3 hexagonal prisms, truncated cubes, and pseudo spheres with corresponding flat projections. Reproduced with permission.[15] Copyright 2014, American Chemical Society. B) Absorbance spectra of $Cu_{2-x}S$ nanodisk with two planes (top) and schematic LSPRs dependence on aspect ratio. Reproduced with permission.[24] Copyright 2012, American Chemical Society. C) Schematic of CuS nanoparticles with different packing orientations for nanodisks (top) and absorbance spectra of the nanodisks with stacked (red) and side-by-side (blue) orientation (bottom). Reproduced with permission.[39] Copyright 2012, Royal Society of Chemistry.

cations and the high activation energy required.[26] As a result, CuS behavior is more metallic in nature and is an unconventional vacancy-undoped chalcogenide. The difficulty in synthesizing CuS is the reason why their optical properties have not been well studied. However, hexagonal disks have been synthesized colloidally[26] with lengths tunable from 10–28 nm with a constant ca. 5 nm height. Two LSPR peaks are expected from the in-plane and out-of-plane surfaces in CuS, as with Cs_xWO_3 hexagons and $Cu_{2-x}S$ disks, but in this instance only one peak is observed. Discrete dipole approximation (DDA) calculations suggest that the energy of the in-plane plasmon has an intensity so much smaller than the out-of-plane plasmon that the latter resonance only produces a minor, hardly recognizable feature with the large aspect ratio of the hexagonal disks.[27] Similar plasmonic absorption features have been observed by Manna et al. in copper phosphide platelets[28] and by Liu et al. in covellite CuS disks.[27] In these two instances, increased aspect ratios result from the in-plane surface of the particles expanding equally in all directions. However, in the $Cu_{2-x}S$ discs described by Hsu et al.,[24] the larger aspect ratio is a result of the particle size elongating more in one direction. This creates a more oval-like shape and the properties behave more like nanorods of Au[21] and Ag,[22] with two distinct LSPR modes visible in the optical spectra.

2.1.5. Indium-Doped Cadmium Oxide Spheres and Octahedrons (ca. 2500 and 3900 nm Absorbance)

As seen in the work of Gordon et al., the plasmon features of indium-doped cadmium oxide (ICO) result from substitutional doping, where indium atoms replace some of the cadmium atoms in the crystal structure, and the shape control is entirely temperature-dependent.[29] As expected, the octahedron ICO has two LSPR features in the NIR (2507 nm and 3898 nm) that become one peak (3296 nm) when in a spherical morphology. This follows the same trend observed in Cs_xWO_3 and is in agreement with the Drude-like free electron model of ICO described by Agrawal et al.,[19] which uses Lorentz–Mie theory and DDA to predict LSPR properties based on particle shape and free-carrier concentration.

2.1.6. Copper–Tin–Selenide Nanosheets, Dots, and Tetrahedra (990–2500 nm)

Another novel class of plasmonic chalcogenides, the copper–tin–selenide (CuSnSe) system described by Wang et al., has a LSPR that may be tuned over a very broad range in the optical spectrum.[30] The absence of Sn produces nanospheres while varying the other reaction conditions results in nanosheets or tetrehedrons. In this system, Sn, reactant selection, and temperature all play important roles in controlling the nanocrystal morphology. Increasing the nanosheet size causes a red shift of a very broad LSRP (beyond 2500 nm). The dots and tetrahedral nanocrystals have much narrower absorbance bands tunable from 1235–1700 nm by varying the ratio of Cu to Sn. Increasing the Sn concentration broadens and redshifts the plasmon until it is no longer visible, where the dampening of the LSPR is due to the dramatic decrease in free hole concentration as the cation vacancies are partially filled by Sn ions.

2.1.7. Synthesis using a Metal Ion Catalysts

Another non-traditional method for controlling chalcogenide morphology is using metal ions as catalysts to control the shape of semiconductor nanoparticles.[31] When Al^{3+} (from aluminum nitrate) is included in the reaction, Cu_3Se_2 nanocubes form with no Al^{3+} detectable by energy dispersive X-ray analysis.[31] The Al^{3+} ion promotes crystal growth in one specific direction and the cubic morphology occurs quickly. The LSPR peak is composition-dependent, and may be tuned from 900 nm to 1100 nm by controlling the shape. It is hypothesized that the nanocubes form during ripening as a result of a stability differential between the different facets.

2.2. Synthetic Routes to Compositional Control in Alloys

In recent years, researchers have discovered advantages to combining metal chalcogenides into alloys, allowing the plasmonic features of separate chalcogenides to be combined in a single nanocrystalline structure. For example, Liu et al. describes quasi-spherical copper–sulfide–selenide ($Cu_{2-x}S_{1-y}Se_y$) nanocrystal alloys with tunable compositions and sizes, whose copper vacancies are responsible for strong near-IR (NIR) LSPR.[32] The Se content plays an important role in determining the position of the LSPR, where the plasmon peak blueshifts with increasing Se content regardless of the change in copper vacancies. This is a result of fundamental differences between $Cu_{2-x}S$ and $Cu_{2-x}Se$. The plasmon peak of the $Cu_{2-x}Se$ nanocrystals is generally stronger and at higher energy than $Cu_{2-x}S$ for the same cationic vacancy concentration. Controlling reaction conditions allows the LSPR to be tuned over a spectral range of 1135–1650 nm, while changing the composition from binary $Cu_{2-x}S$ to ternary $Cu_{2-x}S_{1-y}S_y$ allows the LSPR to be tuned over a broader spectral range (975–1650 nm).

$Cu_{2-x}S$ spheres are also described in the work of Salandha et al., in which copper selenide and copper telluride exhibit alloyed composition with the inclusion of sulfur: $Cu_{2-x}Se_yS_{1-y}$ and $Cu_{2-x}Te_yS_{1-y}$.[33] The LSPR of these materials is widely tunable by controlling oxidation-generating Cu vacancies. The broad LSPR band observed of $Cu_{2-x}S$ shifts from 2400 nm to 1279 nm after oxidation, and a blueshift is also observed when oxidizing $Cu_{2-x}Se_yS_{1-y}$ (1700 nm to 1300 nm) and $Cu_{2-x}Te_yS_{1-y}$ (1000 nm to 600 nm). Despite the alloyed compositions, the particles of both systems exhibit LSPR in the regions characteristic for the corresponding pure binary compounds reported in the literature, which is the same as what was observed in the $Cu_{2-x}S_{1-y}Se_y$ mentioned in the previous paragraph. Interestingly, transition of the oxidized $Cu_{2-x}S$ crystal structure to the roxbyite phase by aging is proven to release copper vacancies without changing the particle size or shape, which influences the position of the LSPR peak. This suggests that the control over crystal structure is an important tool for tuning the plasmonic properties of copper chalcogenide nanocrystals.

Adv. Mater. **2015**,
DOI: 10.1002/adma.201502218

There are several other chalcogenide alloys mentioned in the literature, and for the sake of space in this Research News article only one more will be mentioned here. Liu et al. discuss spherical Cu–Sn–S nanoparticles whose LSPR can be tuned from ca. 1320 nm to 1500 nm by varying the ratio of Cu:Sn.[34] The change in composition causes a change in the carrier density or doping level. This further demonstrates how it is possible to control doping levels in chalcogenide alloys and adds to the ever-increasing size of the toolbox available to researchers seeking to tune plasmonic properties.

2.3. Plasmonic Control Beyond Direct Synthesis

2.3.1. Cation Exchange

It is interesting to note that the cations in a plasmonic metal chalcogenide may be changed after the initial synthesis through cation exchange. This has been reported by several groups in recent years, and the examples mentioned here are only a small sampling of the work that has been done. For example, Ha et al. reported that in copper sulfide spheres ($Cu_{1.81}S$) it is possible to exchange the Cu ion with Zn, without altering the morphology of the nanoparticle.[35] The exchange allows ZnS to replace copper sulfide on the surface. Controlling the extent of cation exchange between Cu and Zn allows the plasmon to be tuned over a broad range of wavelengths, from ca. 1300 nm in copper sulfide to ca. 2300 nm when ZnS replaces all but a thin layer of copper sulfide.

Lesnyak et al. colloidally synthesized copper selenide sulfide ($Cu_{2-x}Se_yS_{1-y}$) platelets and performed an in situ cation exchange to partially replace Cu ions with Zn or Sn, without altering the size or shape of the particles.[36] Unlike the case of ZnS replacing copper selenide, the intensity of the plasmon at ca. 2100 nm (attributed to the oscillation of holes from Cu vacancies) in this system significantly decreases after cation exchange. The plasmon is suppressed by the incorporation of the guest cation, filling the copper vacancies that are responsible for the plasmon. It is possible to engineer the band gap of these nanocrystals, making these materials an available choice for light absorbing applications (e.g., solar cells).

There are several more examples in the literature of cation exchange in plasmonic chalcogenides, including the work of Deka et al. using Cd ion exchange in octapod copper selenide[37] and the work of Luther et al. synthesizing Cu_2S nanocrystals by the cation exchange of CdS nanorods.[38] In addition to size and morphology, cation exchange is another useful tool for tuning the plasmon of metal chalcogenides.

2.3.2. Oriented Assemblies of Plasmonic Nanoparticles

Though often difficult to distinguish in materials like CuS, nanoparticle disks do have two LSPR absorbance peaks corresponding to their in-plane and out-of-plane surfaces. It is possible to orient the direction of the disks via self-assembly, further tuning the LSPR post-synthesis as reported for $Cu_{2-x}S$,[24] ICO,[29] and CuTe.[18] LSPR coupling occurs due to Coulomb interactions between nearest-neighbor nanodisks, and the coupling strength is highly dependent upon disk orientation and carrier density.[39] Though the particle shape does not change during self-assembly, orienting the particles so one face is more prevalent versus the other does influence the plasmon.

In degenerately doped $Cu_{2-x}S$ colloidal disks, Hsu et al. report that particle surfaces may be chemically modified to be hydrophilic or hydrophobic.[39] Through dip-coating, the particles self-assemble and orient themselves either into stacks or in a side-by-side fashion depending upon ligand selection (Figure 2C). Mentioned above, as-synthesized CuS hexagonal disks exhibit only one obvious absorbance peak corresponding to the in-plane LSPR mode. When made hydrophobic and assembled into stacks, the out-of-plane LSPR appears as the dominant mode, while a side-by-side orientation red-shifts the in-plane LSPR. This strong particle orientation-dependence is also observed in $Cu_{1.96}S$ and $Cu_{7.2}S_4$[39] with peak shifts and relative intensities changing when assembled after surface treatment. The ability to tune the LSPR via self-assembly has the potential to create sophisticated metamaterials or to be directly integrated into optical devices.

2.3.3. Ligand Exchange

Post-synthesis, it is also possible to perform a ligand exchange to control the carrier density in heavily doped semiconductor nanocrystals; in noble metal particles, ligand binding generally has a negligible effect on the overall carrier density. This technique has been studied by Balitskii et al. in $Cu_{2-x}Se$, whose copper deficiency provides p-type doping.[40] Attaching electron trapping or donating ligands makes it possible to tune the LSPR over 200 nm (1000–1200 nm), confirming that LSPR is sensitive to the functional groups of attached ligands. This work may lead to the development of new sensing applications in chalcogenides.

Another example of ligand exchange was recently published by Wei et al. on CuS nanodisks, demonstrating a reversible LSPR shift corresponding to oxygen exposure and ligand repassivation.[41] The presence or lack of oxygen on the particle surface controls the position of the plasmon, where adding oxygen to the surface blue-shifts the peak from 1260 nm to 1130 nm. The physical mechanism behind this reversible shift is due to the restoring processes of electrons on the surface, and may open doors to new optical applications for nanocrystalline semiconductors.

3. Compositional Tunability of Nanoparticle Plasmons

The carrier density of metal oxides and chalcogenides may be modulated by tuning their composition.[42] Line phases and non-stoichiometric forms of oxides and chalcogenides are particularly appealing in this respect as their carrier density may be tuned by inserting and extracting either the cations or anions from the lattice. An example of this is the work of Dorfs et al., where the oxidation/reduction of $Cu_{2-x}Se$ nanocrystals changes copper deficiencies and thus the plasmon resonance shape and position.[42] To maintain charge neutrality, the extraction of cations from the lattice is accompanied by the removal of

an electron, leaving behind a valence band hole; similarly, the extraction of anions from the lattice involves placing an electron in the conduction band. Increasing the hole and electron carrier density causes an optical blue-shift of the plasmon energy, linking a chemical event involving ion extraction to an optical observable. The reverse process, insertion of ions, results in a red-shift of the plasmon frequency.

Copper chalcogenides, $Cu_{2-\gamma}X$ (where X = S, Se, or Te) have been extensively explored as hosts of compositionally tunable plasmons.[8,38] With increasing copper deficiency, the carrier density increases and the surface plasmon frequency shifts to higher energies (**Figure 3**A). Cu may be inserted and extracted at room temperature, enabling active tuning of the plasmon frequency. In platelet-shaped covellite copper sulfide nanocrystals reported by Xie et al., varying the ratio of Cu:S from 1.1:1 to 2:1 post-synthesis changes the structural and plasmonic properties.[43] As S content decreases (Cu content increases), the valency of Cu in the lattice remains close to +1 while the average –1 valency of S gradually changes to –2. The result is that the NIR LSPR band red-shifts and broadens until it disappears. The process could be explained as a reduction of the nanocrystal, with S anions evolving from a –1 to –2 valency in the final Cu_2S.[43] Jain et al. discovered that treating stroichiometric Cu_2S with iodine or amines causes a blueshift in the plasmon energy by facilitating the extraction of copper and generating free holes (Figure 3B).[44] Treating copper sulfide with chemical reductants, such as sodium biphenyl or thiols causes a red-shift in the plasmon by reducing the host lattice, filling the free holes with electrons. This compositional-tunability of the surface plasmon resonance has been observed in many different shapes of particles, including spheres, rods, and disks.[44] The same principle of inserting and extracting cations to drive tunability of the plasmon resonance has also been demonstrated in transition metal oxide hosts.

Several transparent conducting oxides with d_{10} electron configurations have also been explored as compositionally tunable plasmon hosts, heterovalently doped tin oxide and zinc oxide exhibit robust plasmons that can be systematically tuned by changing the extent of heterovalent doping.[45] The high mobility of cadmium oxide has been exploited to generate LSPRs with narrow line-widths[29] and co-doping of fluorine and indium/tin in cadmium oxide has been used to reach higher carrier densities and, hence, higher plasmon energies than previously achieved.[7]

Although the majority of work on semiconductor LSPRs has been conducted on the hosts described above, there have also been efforts in other hosts, including nitrides and phosphides.[28] These hosts further expand the rich interplay between the diverse chemistry of these hosts and their optical resonances.

4. Extrinsic Modulation of Plasmon Modes

Semiconductor chalcogenides and doped metal oxides offer exciting new opportunities to extrinsically control the surface

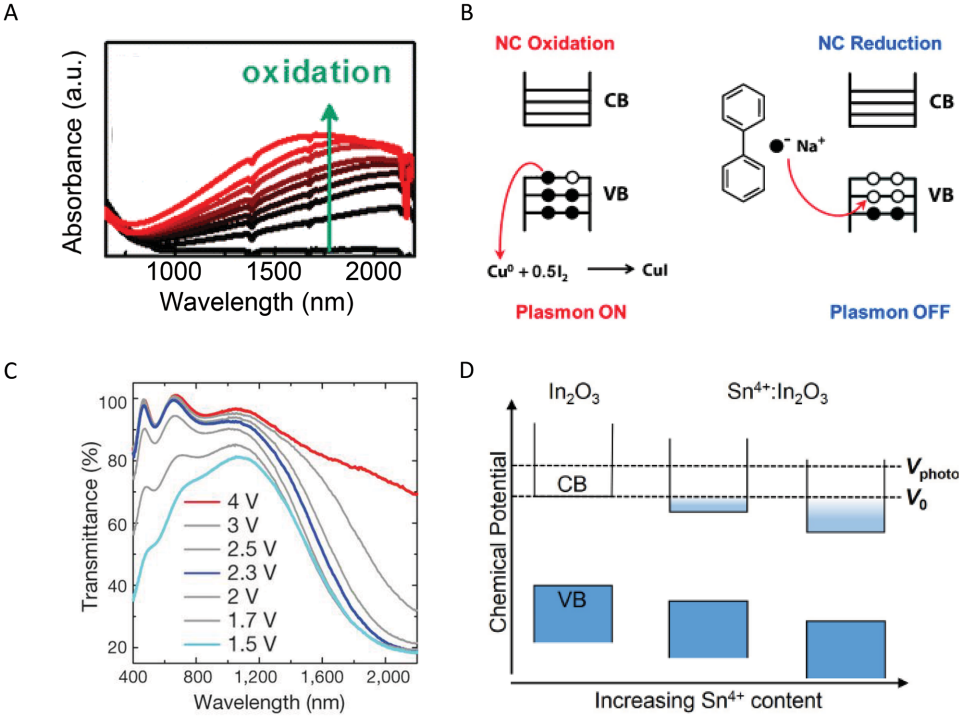

Figure 3. Examples of extrinsic modulation and post-synthetic tuning of the plasmonic response of metal chalcogenide and metal oxide nanocrystals. A) Time evolution of the extinction spectra of $Cu_{2-x}S$ ($x = 0$, black curve) nanocrystals during oxidation in air. Reproduced with permission.[49] Copyright 2012, American Chemical Society. B) Chemical sensitivity of plasmonic $Cu_{2-x}S$ nanocrystals. Reproduced with permission.[44] C) Transmittance spectra of a typical ITO-in-NbO_x film under different applied electrochemical biases (4 V in red, 2.3 V in blue, 1.5 V in cyan, and intermediate voltages shown in grey, versus Li/Li^+). Reproduced with permission.[14] Copyright 2013, Macmillan Publishing Ltd. D) Schematic energy-level diagram showing the effects of added electrons and impurity ions on the plasmon energies in In_2O_3 and ITO nanocrystal. Reproduced with permission.[48] Copyright 2014, American Chemical Society.

Adv. Mater. **2015**,
DOI: 10.1002/adma.201502218

plasmon resonances in a dynamic and often reversible manner. This is difficult to accomplish with traditional noble metal-based plasmonic nanostructures as their high intrinsic carrier density allows for a much weaker effect.[46] The active modulation of plasmonic resonances opens up new technological applications of plasmonics such as electrostatic gating, transparent electrochemical smart windows, and ultrafast optical switches.

Garcia et al. report that the LSPR of doped metal oxide nanocrystals may be dynamically and reversibly tuned by electrochemical modulation of carrier concentrations.[45] The nanocrystal-based electrochromic electrode is shown to be robust upon repetitive charging and discharging. In another demonstration, they used the "nanocrystal-in-glass" approach to achieve unprecedented dynamic optical switching behavior. The ITO nanocrystals embedded in a niobium oxide glass matrix allows independent manipulation of the visible and near-infrared transmittance through the film through electrochemical biasing (Figure 3C), as reported by Llordés et al.[14] Photodoping may also be employed to tune the LSPR, as seen in the work of Schimpf et al. in ZnO[47] and ITO nanocrystals,[48] which allows independent control of the LSPR energies from the initial carrier density introduced through aliovalent doping (Figure 3D).

5. Conclusions

Plasmonic metal chalcogenides have only been studied in the past decade, yet the nature of these materials adds a great deal of control over LSPR absorbance. Researchers now have the opportunity to study plasmon absorbance spanning the entire optical range from infrared to ultraviolet, and independently control the fundamental parameters of carrier mobility and density. Furthermore, semiconductor plasmonic materials are capable of being actively doped or de-doped, enabling both switching applications and also the coupling of enhanced local electric fields to semiconductor band gaps for energy harvesting and generation applications. New methods of intrinsic synthetic control have also evolved, including the ability to use a metal ion as a catalyst to control facets during growth.

Adding ligands to the nanoparticle surface makes self-assembly post-synthesis possible. Hydrophobic ligands enable a plasmonic material to be deposited as films with particles in a stacked orientation, while a hydrophilic ligand results in a side-by-side arrangement. The ability to control the packing of the particles through self-assembly on nanoparticle surfaces makes it possible to observe plasmons resulting solely from the in-plane or out-of-plane surface of the particle. New devices are evolving as new materials emerge, including window coatings to reduce solar heat as well as devices to convert heat to energy. It is now also possible to tune the plasmon through the electrochemical modulation of free electrons.

The discovery of LSPR chalcogenides and metal oxides is quickly advancing energy and optics research. Where will these fields be in another decade? Current research trends already show great potential for these new classes of chalcogenide plasmonic materials in the harvesting of solar energy and the creation of chemical fuels from light, as well as mitigating solar heat gain in buildings with plasmonic nanocrystalline films on windows.

Acknowledgements

This work was completed in part at the Molecular Foundry, Lawrence Berkeley National Laboratory, a user facility supported by the Office of Science, Office of Basic Energy Sciences, of the U.S. Department of Energy (DOE) under contract no. DE-AC02–447 05CH11231 and the Physical Chemistry of Inorganic Nanostructures Program, KC3103, Office of Basic Energy Sciences of the United States Department of Energy under Contract DE-AC02-05CH11232.

Received: May 8, 2015
Revised: June 10, 2015
Published online:

[1] a) H. A. Atwater, *Sci. Am.* **2007**, *296 (April)*, 56; b) M. I. Stockman, *Phys. Today* **2011**, *64 (February)*, 39.
[2] H. A. Atwater, A. Polman, *Nat. Mater.* **2010**, *9*, 205.
[3] a) Y. B. Zheng, B. Kiraly, P. S. Weiss, T. J. Huang, *Nanomedicine (London, UK)* **2012**, *7*, 751; b) K. Yao, Y. Liu, *Nanotechnol. Rev.* **2014**, *3*, 177.
[4] M. S. Tame, K. R. McEnery, S. K. Özdemir, J. Lee, S. A. Maier, M. S. Kim, *Nat. Phys.* **2013**, *9*, 329.
[5] A. Tusboi, K. Nakamura, N. Kobayashi, *Adv. Mater.* **2013**, *25*, 3197.
[6] B. L. Sanchez-Gaytan, Z. Qian, S. P. Hastings, M. L. Reca, Z. Fakhraai, S.-J. Park, *J. Phys. Chem. C* **2013**, *117*, 8916.
[7] X. Ye, J. Fei, B. T. Diroll, T. Paik, C. B. Murray, *J. Am. Chem. Soc.* **2014**, *136*, 11680.
[8] Y. Zhao, H. Pan, Y. Lou, X. Qiu, J. Zhu, C. Burda, *J. Am. Chem. Soc.* **2009**, *131*, 4253.
[9] J. A. Faucheaux, A. L. D. Stanton, P. K. Jain, *J. Phys. Chem. Lett.* **2014**, *5*, 976.
[10] S. D. Lounis, E. L. Runnerstrom, A. Llordés, D. J. Milliron, *J. Phys. Chem. Lett.* **2014**, *5*, 1564.
[11] F. Scotognella, G. D. Valle, A. R. S. Kandada, M. Zavelani-Rossi, S. Longhi, G. Lanzani, F. Tassone, *Eur. Phys. J. B* **2013**, *86*, 1.
[12] X. Liu, M. T. Swihart, *Chem. Soc. Rev.* **2014**, *43*, 3908.
[13] a) B. A. Korgel, *Nature* **2013**, *500*, 278; b) E. L. Runnerstrom, A. Llordés, S. D. Lounis, D. J. Milliron, *Chem. Commun.* **2014**, *50*, 10555.
[14] A. Llordés, G. Garcia, J. Gazquez, D. J. Milliron, *Nature* **2013**, *500*, 323.
[15] T. M. Mattox, A. Bergerud, A. Agrawal, D. J. Milliron, *Chem. Mater.* **2014**, *26*, 1779.
[16] A. Comin, L. Manna, *Chem. Soc. Rev.* **2014**, *43*, 3957.
[17] C. Noguez, *J. Phys. Chem. C.* **2007**, *111*, 3806.
[18] W. Li, R. Zamani, P. Rivera Gil, B. Pelaz, M. Ibáñez, D. Cadavid, A. Shavel, R. A. Alvarez-Puebla, W. J. Parak, J. Arbiol, A. Cabot, *J. Am. Chem. Soc.* **2013**, *135*, 7098.
[19] A. Agrawal, I. Kriegel, D. J. Milliron, *J. Phys. Chem. C* **2015**, *119*, 6227.
[20] I. Kriegel, J. Rodríguez-Fernández, A. Wisnet, H. Zhang, C. Waurisch, A. Eychmüller, A. Dubavik, A. O. Govorov, J. Feldmann, *ACS Nano* **2013**, *7*, 4367.
[21] J. Cao, T. Sun, K. T. V. Grattan, *Sens. Actuators, B* **2014**, *195*, 332.
[22] A. Jakab, C. Rosman, Y. Khalavka, J. Becker, A. Trügler, U. Hohenester, C. Sönnichsen, *ACS Nano* **2011**, *5*, 6880.
[23] K. Manthiram, A. P. Alivisatos, *J. Am. Chem. Soc.* **2012**, *134*, 3995.
[24] S.-W. Hsu, W. Bryks, A. R. Tao, *Chem. Mater.* **2012**, *24*, 3765.
[25] K. L. Kelly, E. Coronado, L. L. Zhao, G. C. Schatz, *J. Phys. Chem. B* **2003**, *107*, 668.
[26] Y. Xie, L. Carbone, C. Nobile, V. Grillo, S. D'Agostino, F. Della Sala, C. Giannini, D. Altamura, C. Oelsner, C. Kryschi, P. D. Cozzoli, *ACS Nano* **2013**, *7*, 7352.

[27] M. Liu, X. Xue, C. Ghosh, X. Liu, Y. Liu, E. P. Furlani, M. T. Swihart, P. N. Prasad, *Chem. Mater.* **2015**, *27*, 2584.
[28] G. Manna, R. Bose, N. Pradhan, *Angew. Chem. Int. Ed.* **2013**, *52*, 6762.
[29] T. R. Gordon, T. Paik, D. R. Klein, G. V. Naik, H. Caglayan, A. Boltasseva, C. B. Murray, *Nano Lett.* **2013**, *13*, 2857.
[30] X. Wang, X. Liu, D. Yin, Y. Ke, M. T. Swihart, *Chem. Mater.* **2015**, *27*, 3378.
[31] W. Li, R. Zamani, M. Ibáñez, D. Cadavid, A. Shavel, J. R. Morante, J. Arbiol, A. Cabot, *J. Am. Chem. Soc.* **2013**, *135*, 4664.
[32] X. Liu, X. Wang, M. T. Swihart, *Chem. Mater.* **2013**, *25*, 4402.
[33] P. L. Saldanha, R. Brescia, M. Prato, H. Li, M. Povia, L. Manna, V. Lesnyak, *Chem. Mater.* **2014**, *26*, 1442.
[34] X. Liu, X. Wang, M. T. Swihart, *Chem. Mater.* **2015**, *27*, 1342.
[35] D.-H. Ha, A. H. Caldwell, M. J. Ward, S. Honrao, K. Mathew, R. Hovden, M. K. A. Koker, D. A. Muller, R. G. Hennig, R. D. Robinson, *Nano Lett.* **2014**, *14*, 7090.
[36] V. Lesnyak, C. George, A. Genovese, M. Prato, A. Casu, S. Ayyappan, A. Scarpellini, L. Manna, *ACS Nano* **2014**, *8*, 8407.
[37] S. Deka, K. Miszta, D. Dorfs, A. Genovese, G. Bertoni, L. Manna, *Nano Lett.* **2010**, *10*, 3770.
[38] J. M. Luther, P. K. Jain, T. Ewers, A. P. Alivisatos, *Nat. Mater.* **2011**, *10*, 361.
[39] S.-W. Hsu, C. Ngo, A. R. Tao, *Nano Lett.* **2014**, *14*, 2372.
[40] O. A. Balitskii, M. Sytnyk, J. Stangl, D. Primetzhofer, H. Groiss, W. Heiss, *ACS Appl. Mater. Interfaces* **2014**, *6*, 17770.
[41] T. Wei, Y. Liu, W. Dong, Y. Zhang, C. Huang, Y. Sun, X. Chen, N. Dai, *ACS Appl. Mater. Interfaces* **2013**, *5*, 10473.
[42] D. Dorfs, T. Härtling, K. Miszta, N. C. Bigall, M. R. Kim, A. Genovese, A. Falqui, M. Povia, L. Manna, *J. Am. Chem. Soc.* **2011**, *133*, 11175.
[43] Y. Xie, A. Riedinger, M. Prato, A. Casu, A. Genovese, P. Guardia, S. Sottini, C. Sangregorio, K. Miszta, S. Ghosh, T. Pellegrino, L. Manna, *J. Am. Chem. Soc.* **2013**, *135*, 17630.
[44] P. K. Jain, K. Manthiram, J. H. Engel, S. L. White, J. A. Faucheaux, A. P. Alivisatos, *Angew. Chem. Int. Ed.* **2013**, *52*, 13671.
[45] G. Garcia, R. Buonsanti, E. L. Runnerstrom, R. J. Mendelsberg, A. Llordes, A. Anders, T. J. Richardson, D. J. Milliron, *Nano Lett.* **2011**, *11*, 4415.
[46] A. M. Brown, M. T. Sheldon, H. A. Atwater, *ACS Photonics* **2015**, *2*, 459.
[47] A. M. Schimpf, C. E. Gunthardt, J. D. Rinehart, J. M. Mayer, D. R. Gamelin, *J. Am. Chem. Soc.* **2013**, *135*, 16569.
[48] A. M. Schimpf, S. D. Lounis, E. L. Runnerstrom, D. J. Milliron, D. R. Gamelin, *J. Am. Chem. Soc.* **2014**, *137*, 518.
[49] I. Kriegel, C. Jiang, J. Rodríguez-Fernández, R. D. Schaller, D. V. Talapin, E. da Como, J. Feldmann, *J. Am. Chem. Soc.* **2012**, *134*, 1583.

Adv. Mater. **2015**,
DOI: 10.1002/adma.201502218